

Plasmon-Photon Coupled Modes Lasing in a Silver-Coated Hemisphere

Xue-Peng Zhan, Xu-Lin Zhang, Hong-Hua Fang, Qi-Dai Chen, Huai-Liang Xu,
and Hong-Bo Sun, *Member, IEEE*

Abstract—A metal-coated hemisphere microcavity is realized by a simple self-assembled process. Plasmon-photon hybrid modes are produced by the metallic microcavity, and the lasing wavelength exhibits a blue shift when compared with no-metal cavities. Simulation shows that the blue shift originates from the redistribution of the electric-field intensity in the microcavity. The metal-coated microcavity exhibits excellent lasing performance at room temperature with a quality factor of ~ 2500 , owing to high-smooth surface of the hemisphere. Our findings may provide a promising candidate for fundamental investigation of plasmon and photon modes interaction and cavity electrostatics.

Index Terms—Microresonators, plasma devices.

I. INTRODUCTION

OVER the past decades, enormous attentions have been paid to the whispering gallery (WG) mode microcavities, such as microdisks, microrings, microcylinders and microspheres due to their low optical loss and small mode volume [1]–[5]. The WG mode microcavities have demonstrated to be excellent candidates for fundamental physics investigation as well as for potential applications in areas such as ideal light sources, active filters and photonic sensing devices for label-free detection [6]–[11]. Recently, metal-coated microresonators have attracted extensive interests by their unique characteristics due to the couplings of photon modes and surface plasmon polaritons (SPPs) [12]–[14]. For instance, Noginov *et al.* theoretically investigated the stimulated emission of SPPs in a microcylinder resonator [15]. Min *et al.* demonstrated that SPPs can be supported in a WG mode microcavity by coating noble metal on the surface of a silica resonator [16]. Although a lot of efforts have been devoted to developing hybrid lasing cavities, the reported high quality (Q) hybrid modes lasers remain rare.

In this letter, we report plasmon-photon hybrid modes resonator with high Q factor through a simple and feasible strategy. The produced metal-coated microcavity exhibits

hybrid plasmon-photon modes lasing with a high Q factor of ~ 2500 . The lasing properties from metal-coated cavity and no-metal one have been comparatively investigated in combination with theoretical simulations. It is clearly demonstrated that a transition occurs from the pure dielectric WG photon mode to the hybrid plasmon-photon modes lasing in the metal-coated hemisphere microcavity [17]–[21].

II. DEVICE FABRICATION AND CHARACTERIZATION

The hemisphere microcavity was created by a self-assembly method similar to that in Reference [22], [23]. Briefly, a small amount of dye-doped SU-8 (Rhodamine B, 1.4 wt %) solution formed microdroplets on a hydrophobic substrate, and then they were solidified to be stable hemispheres. In our case, a thin layer of hydrophobic Teflon material, which could reduce the surface energy, was spin-coated on the substrate. To prepare the solution for the creation of the hemispheres, the viscous SU-8 negative photoresist incorporated with Rhodamine B (Rh-B) dye molecules, was dissolved in cyclopentanone. The solution was spread on a fiber tip and transferred onto the hydrophobic surface to form microdroplets. Then samples were heated on a hot plate and exposed under UV light to form stable hemispheres. For the metal-coated microcavities, they were fabricated by evaporating a layer of noble metal on these hemispheres. In the experiment, a commercial 532 nm narrow band-pass filter (NBF) mirror was used as substrate, and silver was vacuum deposited on the surface with thickness of around 10 nm.

For the characterization of lasing properties, an individual microcavity was investigated in a home-build microphotoluminescence (μ -PL) system. A picosecond laser with wavelength of 532 nm (frequency doubled from a Nd:YLF laser, pulse-width of 15 ps, repetition rate of 50 KHz) was used as excitation source. The pump direction is through the substrate toward the center of the hemispheres. An electric shutter was used to control each expose time of 20 ms to reduce the bleaching effect of the Rh-B dye molecules. To vary the pumping pulse energy, a neutral attenuator was used. The output emitting light was split into two parts: one was collected by a charge-coupled-device (CCD) connected with a spectrometer and the other was brought into a CCD camera for imaging.

III. RESULTS AND DISCUSSIONS

Shown in Fig. 1(a) is the fluorescence microscope image of a microcavity without metal-coater. According to the atomic

Manuscript received August 6, 2015; revised October 22, 2015; accepted October 26, 2015. Date of publication November 9, 2015; date of current version December 23, 2015. This work was supported in part by the National Basic Research Program of China under Grant 2014CB921302, in part by the National Natural Science Foundation of China under Grant 61435005, and in part by the National Natural Science Foundation of China under Grant 51335008, Grant 61127010, and Grant 61137001. (*Corresponding authors: Hong-Hua Fang and Hong-Bo Sun.*)

The authors are with the State Key Laboratory on Integrated Optoelectronics, College of Electronic Science and Engineering, Jilin University, Changchun 130012, China (e-mail: honghua.fang@gmail.com; hbsun@jlu.edu.cn).

Color versions of one or more of the figures in this letter are available online at <http://ieeexplore.ieee.org>.

Digital Object Identifier 10.1109/LPT.2015.2496225

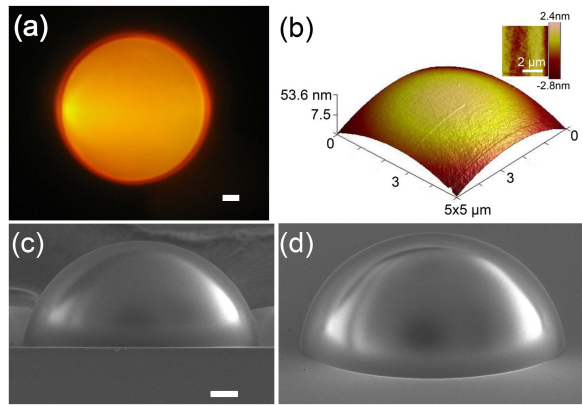


Fig. 1. (a) The optical microscope image of the hemisphere. (b) The top view AFM photograph of the hemisphere, showing the roughness of 0.83 nm. (c) The side view SEM and (d) 75° tilt view SEM of the hemisphere. The same scale bar of 10 μm .

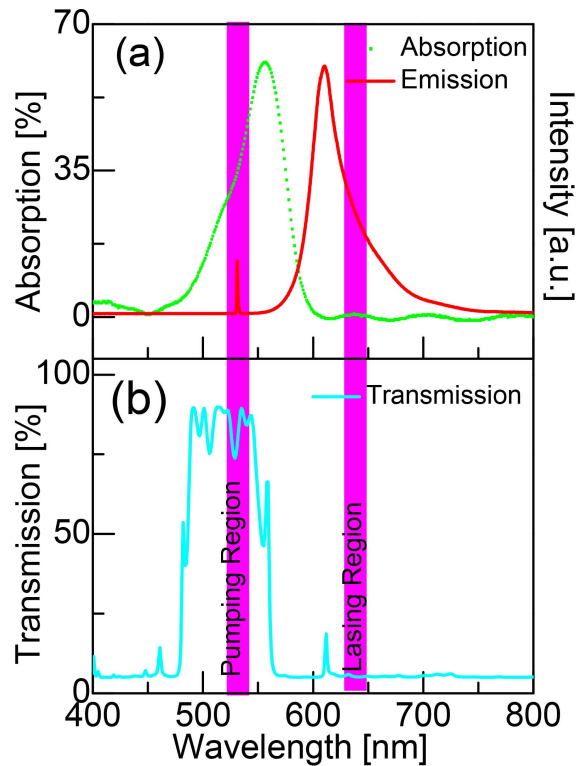


Fig. 2. (a) The absorption and fluorescence emission intensity of the dye-doped epoxy resin solution, with the pumping wavelength of 532 nm (sharp peak). (b) The transmittance of the NBF substrate.

force microscopy (AFM) photograph in Fig. 1(b), the roughness of hemisphere surface is only about 0.83 nm, confirming the priority of self-assembled method. The use of hydrophobic Teflon on the substrate could help to improve the contact angle to 83° as shown in Fig. 1(c) and Fig. 1(d). Fig. 2 shows the absorption and photoluminescence (PL) spectra of the gain materials (Rh-B doped SU-8) as well as the transmitted spectrum of NBF mirror. As the dashed line shown in Fig. 2(a), the absorption peak is around 550 nm, which was measured by a Shimadzu UV-3600 spectrophotometer. Meanwhile,

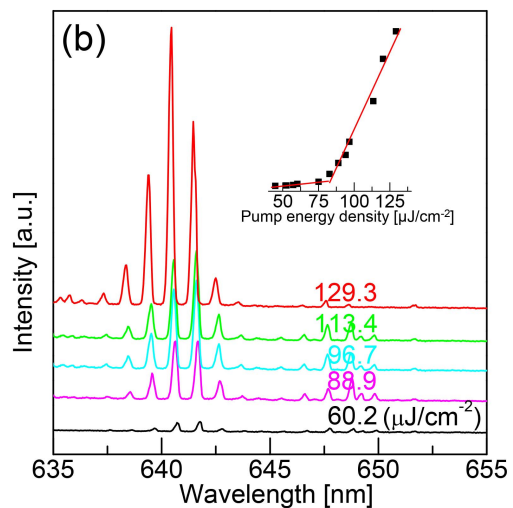
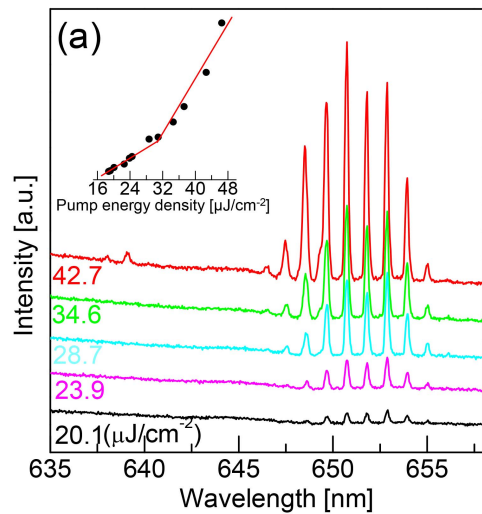


Fig. 3. The emission spectrum of the hemisphere microcavity laser at room temperature without (a) and with (b) metal-cover. Insets are the lasing emitting threshold energy before (a) and after (b) coating metal.

it shows a PL spectra ranging from about 580 nm to 700 nm, when pumped by a picosecond laser with the wavelength of 532 nm corresponds to the sharp peak in the pumping region. The PL spectrum here is related to the optical gain. The substrate acts as a mirror at the PL range for efficient restriction of the emitting light, while it is transparent for the laser (532 nm). As a result, the excitation light can be injected into the microcavity efficiently, while the emission photons are well confined in cavity because of the total internal reflection along the hemisphere as well as the high reflection at surface of NBF substrate.

Prior to investigation of the lasing characteristic of the metal-microcavities, hemispheres without silver were studied. Fig. 3(a) depicts the room temperature lasing emitting spectrum of a single hemisphere microcavity. Multiple sharp peaks emerge from the broad spontaneous range. After reaching the lasing energy threshold, some certain modes are selected and enhanced, whose intensities increase rapidly with further increasing of the pumping pulse energy. The lasing spectrum is affected by not only the gain of materials, but also the

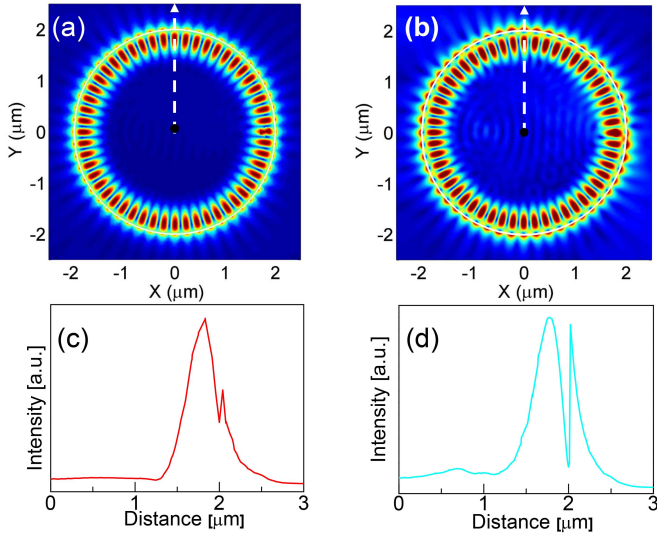


Fig. 4. The simulated spatial mode field distribution of the microcavity without (a) and with (b) the cover silver film. The intensity of the electric field along the dashed line of the microcavity without (c) and with (d) the cover silver film. The same radius of the hemisphere of $2 \mu\text{m}$.

losses in resonator structure. In the micro-hemisphere cavity, the substrate acts as a mirror at the PL range for efficient restriction of the emitting light, which may distort the gain spectrum and shift the lasing wavelength from highest gain to lasing region. The characteristic of the lasing action is investigated by examining the free spectral range (FSR), which is defined as $\Delta\lambda = \lambda^2/\pi nd$, where n is the refractive index and d is the diameter. In this case, the calculated FSR is about 1.00 nm for the hemisphere with $d = 84.5 \mu\text{m}$ and $n = 1.60$ at the wavelength of 650.7 nm , which matches well with the experimental value of 1.06 nm , indicating that the SU-8 hemisphere microcavity has exhibited a pure WG mode of the photon's total internal reflection at the hemisphere-air interface.

Upon a thin film of silver was thermally evaporated onto the hemisphere surface, the lasing emitting spectrum of the microcavity was modulated, as shown in Fig. 3(b). The number of lasing modes is reduced, whereas the experimental FSR does not change in comparison to that of the pure dielectric microcavity. Interestingly, the wavelength of the primary lasing mode has exhibited a blue shift from 650.7 nm to 641.6 nm , corresponding to an energy shift of about 27 meV . And this may be attributed to the change from pure photon mode to hybrid plasmon-photon modes at the silver-air interface with a shift to higher lasing energies, as similarly discussed in Refs [24]–[26].

To further verify this hypothesis, a Finite-Difference Time-Domain (FDTD) simulation was applied to study the mode profile in the microcavity. In a two-dimensional simulation, the diameter was chosen as $4 \mu\text{m}$ to simplify the calculation process. A dipole source was adopted to excite all the modes with sufficient intensity and a collection position was located at the boundary of the microcavity. It is schematically drawn in Fig. 4(a), the calculated electric field distribution ($|E|$, V/m) in the dielectric microcavity. The simulated result

indicates the excitation of a WG photon mode as a result of the total reflection at the dielectric and air interface. With a 10 nm thick silver film, as shown in Fig. 4(b), a redistribution of the electric field can be found, especially at the metal and dielectric interface where the field is strongly localized, and therefore induces a shift of the mode energy. In the time domain FDTD simulation, the dipole source located at the boundary of the microcavity was adopted with the mesh grids of 100 nm . The asymmetric distribution of the dipole source may affect the spatial mode intensity, leading to a slightly asymmetric pattern in Figs. 4(a)–4(b). From the simplified simulated spatial mode field distribution, we can extract the azimuthal mode number m . For $m = 54$, the resonant wavelength of the dielectric and the metallic microcavity are 645 nm (Fig. 4(a)) and 630 nm (Fig. 4(b)), respectively. Such blue shift of the resonance in simulation has agreed with that in the experimental results. These redistributions of the electric field intensity are also shown in Figs. 4(c)–4(d) along the radius direction (as the dashed line) of the microcavity. The strongly enhanced field intensity at the outer silver interface supports our viewpoint of the excitation of the hybrid plasmon-photon modes in the metallic microcavity.

Additionally, the dissipative effect of the coated silver was observed by detecting the lasing threshold energy in both cases. In the pure dielectric microcavity, the lasing threshold energy is around $31.2 \mu\text{J}/\text{cm}^2$. The Q factor can be calculated by $Q = \lambda/\delta\lambda$, with λ and $\delta\lambda$ being the peak wavelength and the full width at half maximum (FWHM), respectively. According the lasing spectrum in Fig. 3(a), the calculated Q factor of the SU-8 microcavity is ~ 3000 at the wavelength of 650.7 nm with the FWHM of 0.22 nm . Whereas the lasing threshold is largely increased by the losses of the surface coating silver, and lasing threshold energy of the metallic microcavity is $82.5 \mu\text{J}/\text{cm}^2$. Meanwhile, the Q factor of the metallic hemisphere microcavity decreases to ~ 2500 at the wavelength of 641.6 nm with the FWHM of 0.26 nm , as shown in Fig. 3(b), but still larger than the value reported in previous works based on hybrid plasmon-photon modes in a metallic microcavity [14].

IV. CONCLUSIONS

In conclusion, metal-coated hemisphere microcavities have been successfully realized with a feasible technique. Lasing modes from both silver-coated and uncoated cavities have been observed. Their lasing properties were comparatively investigated. The blue shift lasing light and increasing in optical loss phenomenon supported the hybrid plasmon-photon modes oscillating within the metallic microcavity. Owing to the simple, high Q resonating property and 3D confinement, the silver-coated hemisphere microcavity provides a promising candidate for fundamental investigation of SPP and WG photon mode interaction and potential applications in the field of photonic devices.

REFERENCES

- [1] L. He, Ş. K. Özdemir, and L. Yang, "Whispering gallery microcavity lasers," *Laser Photon. Rev.*, vol. 7, no. 1, pp. 60–82, Jan. 2013.

- [2] K. J. Vahala, "Optical microcavities," *Nature*, vol. 424, pp. 839–846, Aug. 2003.
- [3] T. Harayama and S. Shinohara, "Two-dimensional microcavity lasers," *Laser Photon. Rev.*, vol. 5, no. 2, pp. 247–271, Mar. 2011.
- [4] H.-H. Fang *et al.*, "Whispering-gallery mode lasing from patterned molecular single-crystalline microcavity array," *Laser Photon. Rev.*, vol. 7, no. 2, pp. 281–288, Mar. 2013.
- [5] S.-Y. Lu *et al.*, "Highly stable on-chip embedded organic whispering gallery mode lasers," *J. Lightw. Technol.*, vol. 32, no. 13, pp. 2415–2419, Jul. 1, 2014.
- [6] H.-H. Fang, J. Yang, J. Feng, T. Yamao, S. Hotta, and H.-B. Sun, "Functional organic single crystals for solid-state laser applications," *Laser Photon. Rev.*, vol. 8, no. 5, pp. 687–715, Sep. 2014.
- [7] K. H. Kim *et al.*, "Cavity optomechanics on a microfluidic resonator with water and viscous liquids," *Light, Sci. Appl.*, vol. 2, p. e110, Nov. 2013.
- [8] D. Dai, J. Bauters, and J. E. Bowers, "Passive technologies for future large-scale photonic integrated circuits on silicon: Polarization handling, light non-reciprocity and loss reduction," *Light, Sci. Appl.*, vol. 1, p. e1, Mar. 2012.
- [9] V. S. Ilchenko and A. B. Matsko, "Optical resonators with whispering-gallery modes—Part II: Applications," *IEEE J. Sel. Topics Quantum Electron.*, vol. 12, no. 1, pp. 15–32, Jan./Feb. 2006.
- [10] X. Wu, M. K. K. Oo, K. Reddy, Q. Chen, Y. Sun, and X. Fan, "Optofluidic laser for dual-mode sensitive biomolecular detection with a large dynamic range," *Nature Commun.*, vol. 5, Apr. 2014, Art. ID 3779.
- [11] X.-P. Zhan *et al.*, "Unidirectional lasing from a spiral-shaped microcavity of dye-doped polymers," *IEEE Photon. Technol. Lett.*, vol. 27, no. 3, pp. 311–314, Feb. 1, 2015.
- [12] M. T. Hill *et al.*, "Lasing in metallic-coated nanocavities," *Nature Photon.*, vol. 1, pp. 589–594, Sep. 2007.
- [13] Y.-F. Xiao, Y.-C. Liu, B.-B. Li, Y.-L. Chen, Y. Li, and Q. Gong, "Strongly enhanced light-matter interaction in a hybrid photonic-plasmonic resonator," *Phys. Rev. A*, vol. 85, no. 3, p. 031805, Mar. 2012.
- [14] Y.-L. Chen, C.-L. Zou, Y.-W. Hu, and Q. Gong, "High- Q plasmonic and dielectric modes in a metal-coated whispering-gallery microcavity," *Phys. Rev. A*, vol. 87, pp. 023824-1–023824-9, Feb. 2013.
- [15] J. K. Kitur, V. A. Podolskiy, and M. A. Noginov, "Stimulated emission of surface plasmon polaritons in a microcylinder cavity," *Phys. Rev. Lett.*, vol. 106, p. 183903, May 2011.
- [16] B. Min *et al.*, "High- Q surface-plasmon-polariton whispering-gallery microcavity," *Nature*, vol. 457, pp. 455–458, Jan. 2009.
- [17] J.-M. Pirkkalainen, S. U. Cho, J. Li, G. S. Paraoanu, P. J. Hakonen, and M. A. Sillanpää, "Hybrid circuit cavity quantum electrodynamics with a micromechanical resonator," *Nature*, vol. 494, pp. 211–215, Feb. 2013.
- [18] R. Won, "Photonic circuits: Organic integration," *Nature Photon.*, vol. 2, pp. 388–388, Jul. 2008.
- [19] A. Rottler, M. Bröll, S. Schwaiger, D. Heitmann, and S. Mendach, "Tailoring of high- Q -factor surface plasmon modes on silver microtubes," *Opt. Lett.*, vol. 36, no. 7, pp. 1240–1242, Apr. 2011.
- [20] S.-H. Kwon *et al.*, "Subwavelength plasmonic lasing from a semiconductor nanodisk with silver nanopan cavity," *Nano Lett.*, vol. 10, no. 9, pp. 3679–3683, Aug. 2010.
- [21] M. Khajavikhan *et al.*, "Thresholdless nanoscale coaxial lasers," *Nature*, vol. 482, pp. 204–207, Feb. 2012.
- [22] V. D. Ta, R. Chen, and H. D. Sun, "Self-assembled flexible microlasers," *Adv. Opt. Mater.*, vol. 24, no. 10, pp. OP60–OP64, Feb. 2012.
- [23] V. D. Ta, R. Chen, and H. D. Sun, "Tuning whispering gallery mode lasing from self-assembled polymer droplets," *Sci. Rep.*, vol. 3, Mar. 2013, Art. ID 1362.
- [24] A. Rottler, M. Harland, M. Bröll, M. Klingbeil, J. Ehlermann, and S. Mendach, "High- Q hybrid plasmon-photon modes in a bottle resonator realized with a silver-coated glass fiber with a varying diameter," *Phys. Rev. Lett.*, vol. 111, p. 253901, Dec. 2013.
- [25] J. Gu, Z. Zhang, M. Li, and Y. Song, "Mode characteristics of metal-coated microcavity," *Phys. Rev. A*, vol. 90, p. 013816, Jul. 2014.
- [26] Y.-F. Xiao *et al.*, "High- Q exterior whispering-gallery modes in a metal-coated microresonator," *Phys. Rev. Lett.*, vol. 105, p. 153902, Oct. 2010.